

# PHYSICAL REVIEW LETTERS

VOLUME 66

15 APRIL 1991

NUMBER 15

## Experimental Confirmation of the Scaling Theory for Noise-Induced Crises

John C. Sommerer,<sup>(1),(2)</sup> William L. Ditto,<sup>(3)</sup> Celso Grebogi,<sup>(1),(3)</sup> Edward Ott,<sup>(1)</sup> and Mark L. Spano<sup>(3)</sup>

<sup>(1)</sup>*The University of Maryland, College Park, Maryland 20742*

<sup>(2)</sup>*Applied Physics Laboratory, Laurel, Maryland 20723*

<sup>(3)</sup>*Naval Surface Warfare Center, Silver Spring, Maryland 20903*

(Received 16 January 1991)

We investigate experimentally the scaling of the average time  $\tau$  between intermittent, noise-induced bursts for a chaotic mechanical system near a crisis. The system studied is a periodically driven (frequency  $f$ ) magnetoelastic ribbon. Theory predicts that for deterministic crises where  $\tau$  scales as  $\tau \sim |f - f_c|^{-\gamma}$  ( $f < f_c$ ,  $f = f_c$  at crisis), the characteristic time between noise-induced bursts ( $f \geq f_c$ ) should scale as  $\tau \sim \sigma^{-\gamma} g(|f - f_c|/\sigma)$ , where  $\sigma$  is the noise strength and  $\gamma$  is the same in both cases. We determine  $\gamma$  for the low-noise ("deterministic") system, then add noise and observe that the scaling for  $\tau$  is as predicted.

PACS numbers: 05.45.+b, 05.40.+j

In dissipative, nonlinear dynamical systems it is often found that small changes in a system parameter lead to sudden changes in chaotic attractors. This phenomenon, termed *crisis*,<sup>1</sup> has been observed experimentally in a number of systems.<sup>2-4</sup> Theoretically, a crisis occurs when, as a system parameter  $f$  reaches its critical value  $f_c$ , the chaotic attractor collides with the stable manifold of an unstable periodic orbit; if the unstable orbit lies inside the attractor's basin of attraction, the characteristic change in the attractor is an increase in size. After the crisis, orbits of the dynamical system typically move chaotically for a time as though on the smaller, precrisis attractor, then burst into chaotic motion over a larger region of phase space, then return to the region of the smaller attractor, and so on. Such *crisis-induced intermittency*<sup>5</sup> has an associated characteristic time  $\tau$ , the average time between bursts. For a large class of low-dimensional systems, and for  $f$  just past its critical value, the characteristic time  $\tau$  is predicted to have a power-law scaling,<sup>5,6</sup>

$$\tau \sim |f - f_c|^{-\gamma}. \quad (1)$$

This scaling behavior has been observed experimentally.<sup>3,4</sup>

In a deterministic system before crisis ( $f > f_c$  by convention in this paper), the characteristic time is infinite, because the system trajectory remains forever on the precrisis attractor. However, if some random noise is added

to the system, there is the possibility that the noise will kick the trajectory across the stable manifold of the unstable orbit with which the attractor collides at  $f = f_c$ . Then the trajectory will be similar to an orbit of the post-crisis system; for example, if the deterministic, post-crisis ( $f < f_c$ ) system exhibits intermittent bursts, so will the noisy,  $f > f_c$  system, and there will be a characteristic time between bursts  $\tau$ . Specific examples of such *noise-induced crises* have been studied numerically and analytically.<sup>7,8</sup> Theory shows<sup>8</sup> that for deterministic crises where  $\tau$  scales as in Eq. (1), the characteristic time for the noise-induced crisis scales as

$$\tau \sim \sigma^{-\gamma} g(|f - f_c|/\sigma), \quad (2)$$

where  $\sigma$  is the strength of the noise,  $g$  is a nonuniversal function depending on the system and on the distribution function of the noise, and  $\gamma$  is the critical exponent of the *deterministic* crisis. Because real physical systems are always accompanied by noise, these considerations are an important complication to the experimental investigation of transient chaos and crisis-induced intermittency. We have observed noise-induced intermittent bursts in a variable-noise, nonlinear mechanical system, and have for the first time confirmed experimentally the applicability of scaling law (2) to a physical system. *We calculate the critical exponent  $\gamma$  for the  $f < f_c$  system, using three operationally independent means that produce results in good agreement, and show that the characteris-*

tic time for the  $f > f_c$  system is consistent with a single function  $g$  over a wide range of  $\sigma$  and  $f - f_c$ , when  $\gamma$  is used to scale the results as in Eq. (2).

The experimental system was a gravitationally buckled, amorphous, magnetoelastic ribbon<sup>9</sup> (transversely annealed  $\text{Fe}_{81}\text{B}_{13.5}\text{Si}_{3.5}\text{C}_2$ ,  $3 \text{ mm} \times 65 \text{ mm} \times 25 \text{ }\mu\text{m}$ ), clamped nearly vertically at its base (the ribbon buckled preferentially to one side), and driven parametrically by a time-varying component to an applied magnetic field (Fig. 1). The time-varying component had both a sinusoidal and a random contribution. The random component was given by

$$\xi(t) = \sum_{k=-\infty}^{\infty} a_k \{ \theta(t - k\delta t) - \theta(t - (k+1)\delta t) \},$$

where  $\theta$  is the unit step function,  $\delta t$  is an update interval, and the  $a_k$  are independent, zero-mean Gaussian pseudorandom variables with variance  $\sigma_a^2$ . The update interval  $\delta t = 0.01 \text{ s}$ , which is much less than the ribbon's mechanical response time of  $1.2 \text{ s}$  ( $1/e$  decay of the ribbon's response to a step change in dc magnetic field). The digitally produced pseudorandom variables  $a_k$  passed standard statistical tests for independence and distribution. These conditions guaranteed that  $\xi(t)$  closely approximated Gaussian white noise. The ribbon is made from a new class of amorphous materials that exhibit very large reversible changes in their Young's modulus  $E$  with the application of a small magnetic field (inset, Fig. 1). The oscillating magnetic field changes the stiffness of the ribbon, which therefore buckles to a correspondingly greater or lesser degree. The degree to which the ribbon is buckled is measured by an MTI Fotonics sensor near the base of the ribbon. Additional details of the apparatus are discussed in Refs. 9 and 10. The sensor output, monotonically related to the ribbon curvature, was

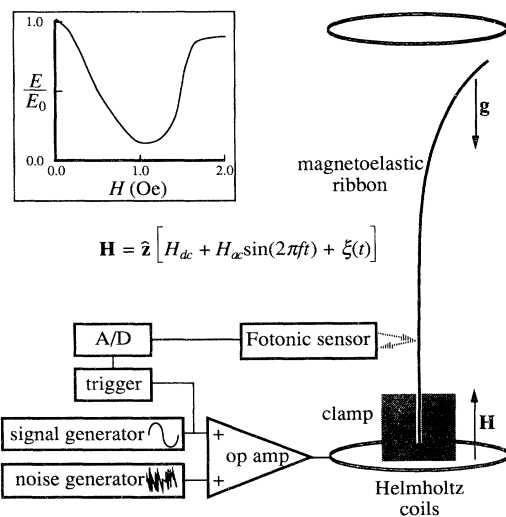


FIG. 1. Experimental setup. Inset: Ratio of Young's modulus  $E$  of the ribbon to zero-field modulus  $E_0$  vs applied magnetic field.

used as the single measured dynamical variable in the experiments. The rest of the system's phase portrait was reconstructed by delay-coordinate embedding.<sup>11</sup> The sensor output-voltage time series was  $V_i = V(t_i)$  ( $t_i = i\Delta t$ ,  $i = 1, 2, 3, \dots$ ;  $\Delta t = 1/f$ , the forcing period). This choice of  $\Delta t$  was made to obtain a stroboscopic Poincaré section in a  $(d+1)$ -dimensional continuous-time phase space. For sufficiently large  $d$ , this choice of  $\Delta t$  induces a discrete  $d$ -dimensional map  $\mathbf{x}_{i+1} = \mathbf{F}(\mathbf{x}_i)$  for the system, where  $\mathbf{x}_i = (V_i, V_{i+1}, V_{i+2}, \dots, V_{i+d})$ . It should be noted that a complete model of the ribbon's behavior requires a partial differential (i.e., infinite-dimensional) equation. It is therefore noteworthy that essential features of the ribbon's dynamics can be captured in a low-dimensional mapping, as has been shown previously.<sup>4,9,10,12</sup>

We observed that for an imposed magnetic field  $H = H_{dc} + H_{ac} \sin(2\pi f t)$  (where  $H_{dc} = 0.82 \text{ Oe}$  and  $H_{ac} = 2.05 \text{ Oe}$ ), as  $f$  decreases through about  $0.97 \text{ Hz}$ , the "deterministic" ( $\xi \equiv 0$ ) system undergoes a crisis. Before the crisis, the system state moves chaotically on a strange attractor [Fig. 2(a)]. After the crisis [Fig. 2(b)], the attractor is much larger. The dynamics during the bursts is more complicated than that between bursts. However, the part of the attractor corresponding to the precrisis attractor (the *core*) is adequately represented in a two-dimensional phase space. Turning on the noise term ( $\xi \neq 0$ ) produces orbits much like those of the post-crisis system, even for  $f > f_c$  [Fig. 2(c)].

The scaling exponent  $\gamma$  of the deterministic crisis was calculated in three operationally independent ways. First,  $\gamma$  was determined by measuring the characteristic time between bursts  $\tau$  as a function of  $f - f_c$ , and fitting the results with Eq. (1). Estimates  $\hat{\tau}$  of  $\tau$  were obtained from 3-h time series recorded for closely spaced values of  $f$  near the crisis ( $\hat{\tau}$  is measured in forcing periods of the sinusoidal magnetic-field component). The theoretical scaling law (1) for  $\tau$  assumes that the system is deterministic; for such a system, the characteristic time goes to infinity at the crisis. Real systems, which are always accompanied by noise, show a finite characteristic time<sup>8</sup> at  $f = f_c$  as is evident from Eq. (2). The presence of residual system noise, even with the  $a_i$  set to zero, made determining the value of  $f_c$  more complicated than in an ideal system, and somewhat limited the accuracy with which it could be determined. The value of  $f_c$  for this crisis was determined by minimizing the degree to which a plot of  $\hat{\tau}$  vs  $\ln(f_c - f)$  deviated from a straight line, using data taken not too near  $f_c$  [where noise strongly affects the applicability of Eq. (1)]. Given  $f_c$ ,  $\gamma$  was determined from the best nonlinear least-squares fit of the functional form  $\hat{\tau} = k(f_c - f)^{-\gamma}$  to the data. The statistical estimate of the critical exponent using this method is  $\gamma = 1.12 \pm 0.02$ .

A second determination of  $\gamma$  was made by considering the accumulation of probability measure at the edge of the attractor. The theory leading to scaling law (1) assumes<sup>5,6</sup> that the measure  $\mu$  of the attractor within  $\epsilon$  of

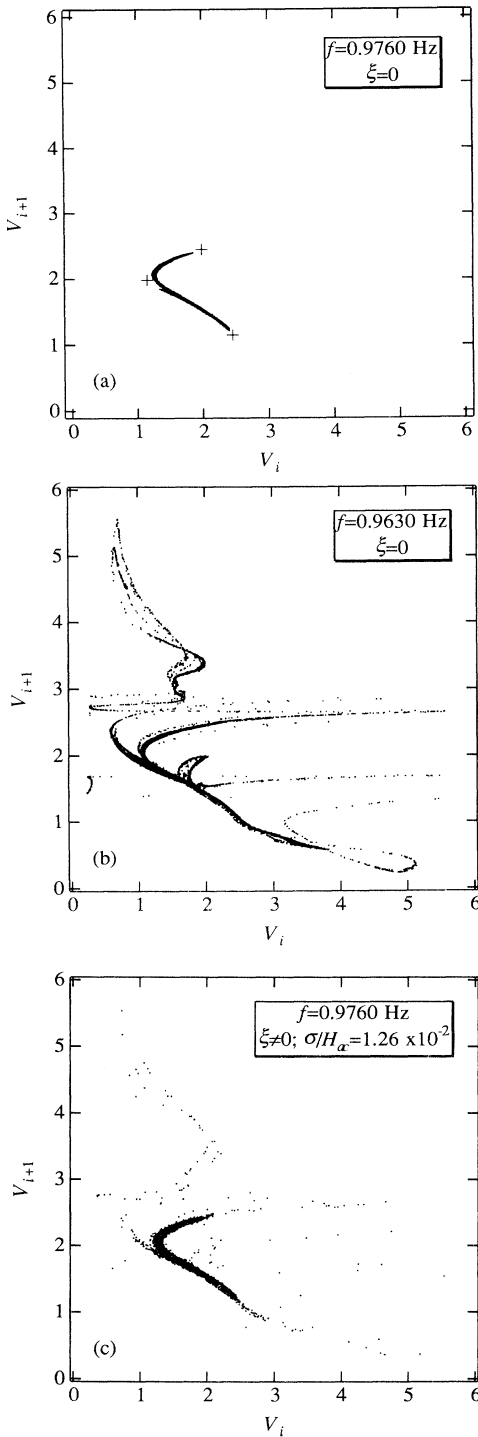


FIG. 2. Delay-coordinate embedding of time series taken (a) before and (b) after the crisis. The time delay  $\Delta t$  is  $1/f$ , the stroboscopic sampling period. The core attractor of (a) is enlarged by burst dynamics in (b). In (c), the parameter is held at the same value as in (a), but the variable noise is on. The noise produces burst dynamics similar to those seen in (b). The small crosses in (a) indicate the elements of the period-three unstable orbit that mediates this crisis.

its edge accumulates as  $\mu(\epsilon) \sim \epsilon^\gamma$ . Using a trajectory of several hours duration recorded for  $f$  just above  $f_c$ , the iterates were sorted in magnitude, and an estimate of  $\mu(\epsilon)$  was obtained as a cumulative count of the number of iterates within  $\epsilon$  of the maximum iterate. The slope of the straight-line portion of a plot of  $\ln[\mu(\epsilon)]$  vs  $\ln(\epsilon)$  produced an estimate of  $\gamma = 1.08 \pm 0.05$ .

Final determination of  $\gamma$  resulted from the observation that the crisis shown in Fig. 2 is a homoclinic tangency crisis of a two-dimensional map. Careful observation of the system state just before a burst indicated that system trajectories closely approached a period-three orbit [the elements of which are indicated in Fig. 2(a)] before leaving the core attractor. Crises in two-dimensional maps are limited to two varieties, depending on whether the mediating periodic orbit is on the attractor before (heteroclinic) or only just at and after (homoclinic) the crisis.<sup>5,6</sup> The absence of a period-three orbit on the attractor before the crisis means that the crisis is of the homoclinic type. The theoretically predicted critical exponent for a homoclinic tangency crisis is given<sup>5,6</sup> by  $\gamma = \log|\beta_2|/2 \log|\beta_1\beta_2|$ , where  $\beta_1$  and  $\beta_2$  are the expanding ( $|\beta_1| > 1$ ) and contracting ( $|\beta_2| < 1$ ) eigenvalues, respectively, of the periodic orbit. Using portions of a single trajectory passing near the period-three orbit, we were able to estimate the eigenvalues  $\beta_1$  and  $\beta_2$ , and, consequently, the theoretically predicted exponent,<sup>4</sup>  $\gamma = 1.07 \pm 0.15$ . These three estimates of  $\gamma$  are statistically consistent, and yield an overall, weighted value of  $\gamma = 1.11 \pm 0.02$ .

The residual system noise mentioned above (resulting from mechanical vibrations and imperfections in the operational amplifier) must be taken into account when applying Eq. (2), in which the strength  $\sigma$  of the total noise experienced by the system appears. We allowed

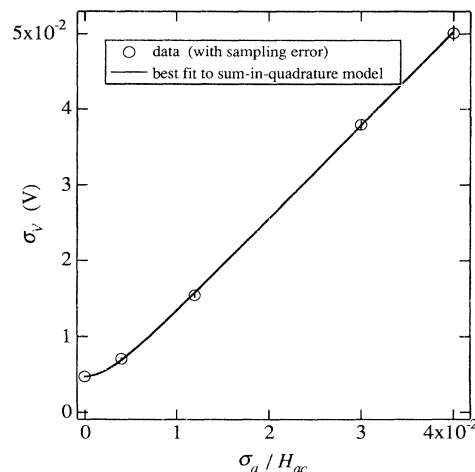


FIG. 3. Measured standard deviation of the iterate sequence  $V_i$  as a function of the strength of the added noise. Here, the system's attractor is a stable periodic orbit. The curve shows the best fit with the sum-in-quadrature model  $\sigma_V = k(\sigma_\delta^2 + \sigma_a^2)^{1/2}$ .

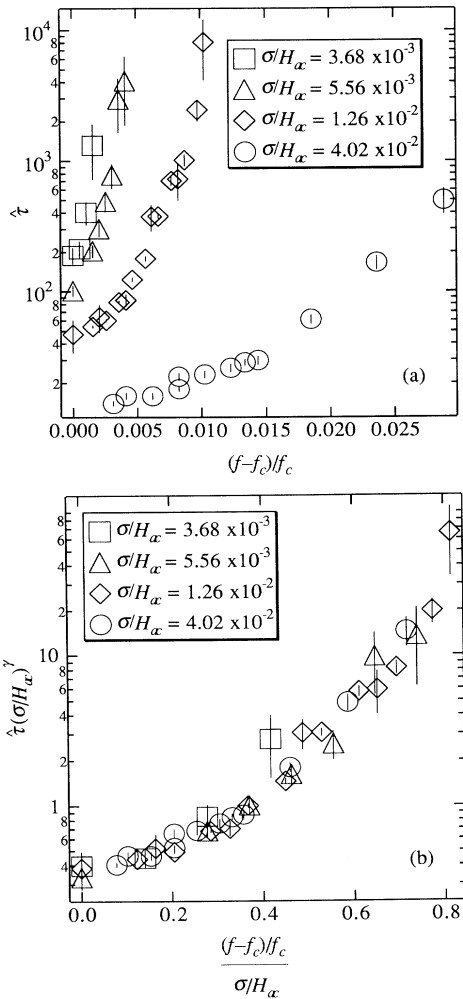


FIG. 4. Characteristic times for noise-induced bursting. (a) Range of raw data. Scaling of Eq. (2) is applied in (b), using deterministic critical exponent  $\gamma$ . Data collapse onto a single curve, giving graph of function  $g$  in Eq. (2). Error bars indicate 67%-confidence intervals. Note that the smallest value of  $\sigma_0/H_{ac}$  corresponds to residual system noise alone.

for this fact as follows. When the system was operated at a different set of parameters ( $H_{dc}=0.22$  Oe,  $H_{ac}=2.05$  Oe,  $f=0.95$  Hz,  $\xi \equiv 0$ ) it was noted that the attractor was not chaotic, but rather was a *stable* periodic orbit. The sequence of iterates  $V_i$  had a Gaussian distribution, due to the system noise, with a standard deviation  $\sigma_V$  of about 5 mV. Spectral analysis of the sensor output voltage  $V(t)$  showed a broadband component even for “periodic” ribbon motion, indicating an approximately white Gaussian process for the residual system noise. As the variable noise was increased ( $\xi \neq 0$ ), the distribution of  $V_i$  remained Gaussian, but broadened. As shown in Fig. 3, the effect of the variable noise on the system state was well described by an additive variance

model, consistent with the residual system noise and the variable noise being independent, white Gaussian processes. In testing the applicability of Eq. (2), we used an effective noise strength  $\sigma = (\sigma_0^2 + \sigma_a^2)^{1/2}$ , where the residual system noise was determined from the fit in Fig. 3 to be  $\sigma_0/H_{ac} = 3.68 \times 10^{-3}$ .

Figure 4(a) shows the characteristic times  $\hat{\tau}$  estimated from data runs taken at a wide variety of noise and (pre-crisis,  $f > f_c$ ) parameter values. In Fig. 4(b), the scaling indicated by Eq. (2) has been applied, using the critical exponent determined for  $f < f_c$  and  $a_k \equiv 0$ . The widely dispersed data of Fig. 4(a) now collapse onto a single curve, which gives the graph of the function  $g$  in Eq. (2) for this system. This consistency strongly supports the theory underlying scaling law (2).

J.C.S. was supported by the U.S. Air Force Office of Scientific Research. Additional support was provided by the U.S. Office of Naval Research (Physics Division), the U.S. Department of Energy (Scientific Computing Staff Office of Energy Research), and the U.S. Naval Surface Warfare Center Independent Research Program.

<sup>1</sup>C. Grebogi, E. Ott, and J. A. Yorke, Phys. Rev. Lett. **48**, 1507 (1982); Physica (Amsterdam) **7D**, 181 (1983).

<sup>2</sup>C. Jeffries and J. Perez, Phys. Rev. A **27**, 601 (1983); S. K. Brorson, D. Dewey, and P. S. Linsay, *ibid.* **28**, 1201 (1983); H. Ikezi, J. S. deGrasse, and T. H. Jensen, *ibid.* **28**, 1207 (1983); E. G. Gwinn and R. M. Westervelt, Phys. Rev. Lett. **54**, 1613 (1985); D. Dangoisse, P. Glorieux, and D. Hannequin, *ibid.* **55**, 746 (1985).

<sup>3</sup>R. W. Rollins and E. R. Hunt, Phys. Rev. A **29**, 3327 (1984); T. L. Carroll, L. M. Pecora, and F. J. Rachford, Phys. Rev. Lett. **59**, 2891 (1987); W. L. Ditto *et al.*, *ibid.* **63**, 923 (1989).

<sup>4</sup>J. C. Sommerer, W. L. Ditto, C. Grebogi, E. Ott, and M. L. Spano, Phys. Lett. A **153**, 105 (1991).

<sup>5</sup>C. Grebogi, E. Ott, F. Romeiras, and J. A. Yorke, Phys. Rev. A **36**, 5365 (1987).

<sup>6</sup>C. Grebogi, E. Ott, and J. A. Yorke, Phys. Rev. Lett. **57**, 1284 (1986).

<sup>7</sup>F. T. Arecchi, R. Badii, and A. Politi, Phys. Lett. **103A**, 3 (1984); R. L. Kautz, J. Appl. Phys. **62**, 198 (1987); P. D. Beale, Phys. Rev. A **40**, 3998 (1989).

<sup>8</sup>J. C. Sommerer, E. Ott, and C. Grebogi, Phys. Rev. A **43**, 1754 (1991).

<sup>9</sup>H. T. Savage and C. Adler, J. Magn. Magn. Mater. **58**, 320 (1986); H. T. Savage and M. L. Spano, J. Appl. Phys. **53**, 8002 (1982).

<sup>10</sup>H. T. Savage *et al.*, J. Appl. Phys. **67**, 5619 (1990).

<sup>11</sup>F. Takens, in *Dynamical Systems and Turbulence*, edited by D. A. Rand and L.-S. Young (Springer-Verlag, Berlin, 1980), p. 366ff; N. H. Packard *et al.*, Phys. Rev. Lett. **45**, 712 (1980).

<sup>12</sup>W. L. Ditto, S. N. Rauseo, and M. L. Spano, Phys. Rev. Lett. **63**, 3211 (1989); W. L. Ditto *et al.*, *ibid.* **65**, 533 (1990).